Journal of Catalysis 279 (2011) 163–173

Contents lists available at ScienceDirect

Journal of Catalysis

journal homepage: www.elsevier.com/locate/jcat

Effect of biomass-derived synthesis gas impurity elements on cobalt Fischer–Tropsch catalyst performance including *in situ* sulphur and nitrogen addition

Øyvind Borg [a], Nina Hammer [a,1], Bjørn Christian Enger [a,1], Rune Myrstad [b], Odd Asbjørn Lindvåg [b], Sigrid Eri [a], Torild Hulsund Skagseth [a], Erling Rytter [a,*]

[a] Statoil Research Center Trondheim, NO-7005 Trondheim, Norway
[b] SINTEF Materials and Chemistry, NO-7465 Trondheim, Norway

ARTICLE INFO

Article history:
Received 14 September 2010
Revised 13 January 2011
Accepted 15 January 2011
Available online 17 February 2011

Keywords:
Biomass-to-liquids
Fischer–Tropsch synthesis
Cobalt
Impurity
Reaction rate
Selectivity
Alkali metals
Alkaline earth metals
Chlorine
Sulphur

ABSTRACT

The effect of 10 typical biomass-derived synthesis gas impurities on cobalt Fischer–Tropsch catalyst performance was investigated at industrially relevant conditions. Impurities (0–1000 ppmw) were introduced *ex situ* by incipient wetness impregnation to give 23 different compositions. The presence of alkali (Na, K) and alkaline earth elements (Ca, Mg) did not affect the *ex situ*-measured cobalt surface area but decreased the *in situ* activity, thereby decreasing the apparent turnover frequency. The C_{5+} selectivity increased and decreased upon addition of alkali and alkaline earth metals, respectively. Mn, Fe, and P had minor effects on catalyst performance. The presence of Cl decreased cobalt surface without affecting activity, thus increasing the turnover frequency. The changes in turnover frequency correlated with element electronegativity. *In situ* addition of H_2S and $(CH_3)_2S$ (2.5–10 ppm) decreased activity at all concentrations. However, product selectivity was not affected. Addition of NH_3 (4 ppm) did not change catalytic performance.

1. Introduction

The term BTL (“biomass-to-liquids”) refers to the production of clean liquid fuels from biomass, a renewable, carbon-containing feedstock. BTL consists of three main steps: synthesis gas generation from biomass (i.e. gasification), Fischer–Tropsch synthesis (i.e. production of long-chain hydrocarbons from synthesis gas), and product upgrading. In addition to the major species CO, CO_2, and H_2, the biomass-derived synthesis gas frequently contains a number of gaseous contaminants. Typical are the organic impurities tars and BTX (benzene, toluene, and xylenes), the inorganic impurities NH_3, HCN, H_2S, COS, and HCl, and furthermore volatile metals, dust, and soot [1]. The composition of the synthesis gas is very dependent on the type of gasification technology and conditions employed. Although present in moderate amounts, the impurities can have a significant impact on the downstream cobalt Fischer–Tropsch catalyst. For this reason, the synthesis gas is carefully cleaned in various steps. There are no definite limits for how clean the synthesis gas must be before it enters the Fischer–Tropsch synthesis reactor. As catalysts are replaced or regenerated after a certain period, the cost of cleaning must be weighed against the loss in production due to poisoning of the catalyst [2]. Note that poisoning can also take place as a malfunction or upset in the operation over a shorter period of time. For these reasons, it is imperative to know how impurities affect the catalyst and how large quantities can be tolerated.

It must be emphasised that impurities do not only originate from the synthesis gas feedstock. For instance, refractory or ceramic materials employed in the synthesis gas generation and cleaning process can be a source of alkali and alkaline earth metals. Carryover of material from these sections can increase the concentration of contaminants in the synthesis gas. Furthermore, alkali and alkaline earth metals can be introduced to the Fischer–Tropsch catalyst in the catalyst preparation steps. These compounds may for instance be introduced via impure water, cobalt and promoter precursors, and process equipment. Common supports also often contain certain amounts of sodium and calcium, inherent from

* Corresponding author. Fax: +47 73 58 49 65.
E-mail address: err@statoil.com (E. Rytter).
[1] Present address: Department of Chemical Engineering, Norwegian University of Science and Technology (NTNU), NO-7491 Trondheim, Norway.

0021-9517/$ - see front matter © 2011 Elsevier Inc. All rights reserved.
doi:10.1016/j.jcat.2011.01.015

the preparation procedure. For a commercial BTL plant, detailed insight into poisoning effects must be established before limits for synthesis gas purity are specified.

This paper investigates the extent to which small amounts (i.e. ppmw levels) of a number of typical biomass-derived synthesis gas impurities (Na, K, Mg, Ca, Mn, Fe, N, P, S, Cl) influence the cobalt Fischer–Tropsch synthesis. A total of 23 catalysts have been prepared, and among these, different supports and different impregnation protocols are represented. The effect of S and N has been studied *in situ* by the addition of H_2S, $(CH_3)_2S$, and NH_3 containing synthesis gases. Most of the mentioned impurity elements have been looked at in the literature, but then mainly as promoters and not as impurity elements. Typical promoter concentrations are significant in this context, and literature data are, therefore, often not directly relevant. For this reason, a thorough literature review is not presented and the interested reader is referred directly to the literature (Na [3–5], K [3,5,6], Mg [7–9], Ca [5], Mn [10,11], Fe [12,13], N [14,15], P [16–18], S [19–24], Cl [2,25]). However, some investigations deserve special attention, and these are commented on in Section 3: Results and discussion.

2. Experimental

2.1. Catalyst preparation

Impurity components can allegedly have a significant adsorption capacity in fixed-bed reactor lines. Therefore, most samples were *ex situ*-modified by impregnation. All *ex situ*-modified catalysts were prepared by one-step incipient wetness impregnation of different supports with aqueous solutions of cobalt nitrate hexahydrate, $Co(NO_3)_2{\cdot}6H_2O$, and perrhenic acid, $HReO_4$. Impurity precursors were either added in the same impregnation step, i.e. co-impregnation, or added at a later stage, i.e. post-impregnation.

When co-impregnation was carried out, the catalysts were dried at 110 °C for 3 h and then calcined at 300 °C for 16 h after impregnation. In the post-impregnation cases, cobalt and rhenium impregnation was followed by drying at 110 °C for 3 h and calcination at 300 °C for 16 h. Impurity precursors were then incipient wetness-impregnated onto the catalysts. Additional drying and calcination finalised the catalyst preparation procedure. Table 1 gives detailed information about all catalysts included in this investigation. Whether the impurities were co-impregnated or post-impregnated can be inferred from the third column of Table 1. The following impurity precursors were used (impurity element given in parenthesis); $NaNO_3$ (Na), $Ca(NO_3)_2{\cdot}4H_2O$ (Ca), KNO_3 (K), $Mg(NO_3)_2{\cdot}6H_2O$ (Mg), $Mn(NO_3)_2{\cdot}6H_2O$ (Mn), $Fe(NO_3)_3{\cdot}9H_2O$ (Fe), H_3PO_4 (P), $CoCl_2{\cdot}6H_2O$ (Cl). Impurity precursors were added in amounts to give from 100 to 1000 ppmw of the impurity element in the final catalyst.

2.2. Catalyst characterisation

2.2.1. Nitrogen adsorption/desorption

Nitrogen adsorption/desorption isotherms were measured on a Micromeritics TriStar 3000 instrument, and the data were collected at liquid nitrogen temperature. The samples (0.3 g, 53–90 μm) were outgassed at 250 °C for 2 h before measurement.

The surface area was calculated from the Brunauer–Emmett–Teller (BET) equation [26], and the total pore volume and pore size distribution were found by applying the Barrett–Joyner–Halenda (BJH) method [27]. The nitrogen desorption branch was chosen for pore size analysis [28].

2.2.2. Hydrogen chemisorption

Hydrogen adsorption isotherms were recorded on a Micromeritics 2020C unit at 40 °C. The samples (0.5 g, 53–90 μm) were reduced *in situ* in flowing hydrogen at 350 °C for 16 h. The temperature was increased by 1 °C/min from room temperature to 350 °C. After reduction, the samples were evacuated for 1 h at 330 °C and for 30 min at 100 °C before subsequently cooling it to 40 °C. An adsorption isotherm was recorded at this temperature in the pressure interval ranging from about 15 to 500 mm Hg. The samples were outgassed at 250 °C for 2 h before measurement.

The amount of chemisorbed hydrogen was determined by extrapolating the straight-line portion of the isotherm to zero pressure. Furthermore, to calculate the dispersion, it was assumed that two cobalt surface atoms were covered by one hydrogen molecule and that rhenium or other elements did not contribute to the amount of hydrogen adsorbed.

2.2.3. Propene chemisorption

Propene chemisorption was used as a second technique for the measurement of the number of active adsorption sites on the catalytic cobalt surface. The experiments were performed on a Micromeritics AutoChem II 2920 unit, and the procedure was adapted from Girardon et al. [29]. The catalyst samples (1.0 g, 53–90 μm) were reduced *in situ* under flowing hydrogen for 16 h at 350 °C. The temperature was linearly ramped from ambient to 350 °C at a rate of 1 °C/min. After reduction, the samples were cooled to 50 °C and flushed in flowing He for 1 h. A series of pulses of propene were passed through the catalyst bed at the same temperature. The amount of propene chemisorbed on the surface was used as a relative measurement of the number of cobalt metal sites present in the reduced cobalt catalysts. It was confirmed in separate experiments that propene did not chemisorb onto the supports.

2.2.4. Oxygen titration

Oxygen titration was used to measure degree of reduction for a selection of samples and was performed on a Micromeritics AutoChem II 2920 unit. The catalyst samples (0.1 g, 53–90 μm) were reduced *in situ* under flowing hydrogen for 16 h at 350 °C. The temperature was linearly ramped from ambient temperature to 350 °C at a rate of 1 °C/min. The samples were flushed in flowing He at 350 °C for 1 h and subsequently heated to 400 °C at 5 °C/min, keeping the same gaseous atmosphere. A series of pulses of oxygen were passed through the catalyst bed at 400 °C [30]. The amount of oxygen consumed by the samples was calculated from the known pulse volume and the number of pulses reacting with the sample. The degree of reduction was calculated assuming that all cobalt in metallic form was oxidised to Co_3O_4. Any oxidation of Re to Re_2O_7 was not considered in the calculations.

2.3. Fischer–Tropsch synthesis

2.3.1. Fischer–Tropsch synthesis without addition of sulphur- or nitrogen-containing compounds

Fischer–Tropsch synthesis was performed in a reactor system containing four parallel, isothermal fixed-bed reactors. The samples (1 g for catalysts containing 20 wt.% Co and 1.67 g for catalysts containing 12 wt.% Co, in both cases 53–90 μm) were diluted with inert silicon carbide (20 g, 75–150 μm) particles. The catalysts were reduced *in situ* in H_2 at 1 bar, while the temperature was increased by 1 °C/min to 350 °C. After 16 h of reduction at 350 °C, the catalysts were cooled to 170 °C. The reactor system was then pressurised to 20 bar, and synthesis gas of molar ratio $H_2/CO = 2.1$ (and 3% N_2 as internal standard) was introduced into the reactor. The pre-mixed synthesis gas was delivered by Yara and did not contain any impurity atoms (gas purity: H_2: 5.0, CO: 3.7, N_2: 5.0). To avoid runaway and subsequent catalyst deactivation at start-up, the temperature was increased slowly to the reaction temperature of 210 °C.

Table 1
Catalyst overview. The catalysts of Series 1, 2, 3, and 6 contain 20 wt.% Co and 0.5 wt.% Re, the catalysts of Series 4 contain 12 wt.% Co and 0.5 wt.% Re, while the catalysts of Series 5 contain 12 wt.% Co and 0.3 wt.% Re.

Support	Impurity type and amount	Impurity co- or post-impregnation	BET surface area (m^2/g)	Pore volume (cm^3/g)	Co surface area (m^2/g)[a]	Amount C_3H_6 chemisorbed (μmol/g)	CO reaction rate (10^{-2} mol CO/(g_{cat} h))	TOF_{H2} (s^{-1})[e]	C_{5+} selectivity (%)[f]	CO_2 selectivity (%)[g]	C_3 olefin/paraffin ratio[h]
Series 1:											
γ-Al_2O_3[b]	0	–	127	0.50	12.2	71	5.9	54	84.4	0.18	2.65
γ-Al_2O_3[b]	100 ppmw Ca	co	138	0.49	12.1	72	5.2	48	83.1	0.21	2.32
γ-Al_2O_3[b]	500 ppmw Ca	co	135	0.48	12.2	72	3.7	34	83.4	0.23	2.24
γ-Al_2O_3[b]	1000 ppmw Ca	co	136	0.48	12.0	71	2.9	26	82.5	0.29	2.13
Series 2:											
SiO_2[c]	0	–	240	0.81	na	na	5.4	na	86.8	0.13	2.62
SiO_2[c]	500 ppmw Ca	co	248	0.80	8.4	na	1.8	24	86.3	0.39	2.69
Series 3:											
γ-Al_2O_3[b]	0	–	na	na	na	na	6.1	na	82.8	0.17	2.43
γ-Al_2O_3[b]	100 ppmw Na	co	na	na	na	na	5.9	na	83.6	0.14	2.39
γ-Al_2O_3[b]	200 ppmw Na	co	na	na	na	na	5.6	na	83.9	0.13	2.54
γ-Al_2O_3[b]	400 ppmw Na	co	na	na	na	na	3.7	na	84.7	0.26	2.64
Series 4:											
TiO_2[d]	0	–	31	0.14	na	na	1.9	na	90.2	0.10	2.58
TiO_2[d]	200 ppmw Na	co	31	0.16	na	na	0.093	na	90.2	0.31	2.60
Series 5:											
$NiAl_2O_4$	H_2O[i]	–	47	0.18	7.3	47	3.4	52	83.1	0.16	2.13
$NiAl_2O_4$	400 ppmw Ca	post	46	0.18	7.1	44	2.0	31	81.0	0.46	2.02
$NiAl_2O_4$	400 ppmw Mg	post	47	0.19	7.0	46	3.1	48	82.2	0.20	2.15
$NiAl_2O_4$	400 ppmw Na	post	44	0.17	7.1	46	1.8	28	84.1	0.35	2.42
$NiAl_2O_4$	400 ppmw K	post	47	0.19	7.1	45	2.5	40	84.2	0.26	2.33
$NiAl_2O_4$	400 ppmw Mn	post	45	0.18	7.1	45	3.3	52	82.8	0.19	2.24
$NiAl_2O_4$	800 ppmw Fe	post	46	0.19	7.1	46	3.3	52	82.0	0.17	2.26
$NiAl_2O_4$	400 ppmw P	post	46	0.18	6.9	41	3.2	51	81.9	0.18	2.07
$NiAl_2O_4$	800 ppmw Cl	post	45	0.19	5.5	35	3.3	67	82.7	0.20	2.13
Series 6:											
γ-Al_2O_3[b]	H_2O[i]	–	na	na	11.9	na	5.1	48	81.1	0.18	2.34
γ-Al_2O_3[b]	1333 ppmw Cl	post	na	na	9.2	na	5.4	66	82.6	0.15	2.40

[a] Determined from hydrogen chemisorption data.
[b] The γ-Al_2O_3 is a Puralox CCa type from Sasol GmbH (BET surface area = 170 m^2/g, pore volume = 0.74 m^3/g).
[c] The SiO_2 is type 432 from Grace GmbH calcined at 500 °C.
[d] The TiO_2 is Degussa P25 type.
[e] Based on hydrogen chemisorption data.
[f] C_{5+} selectivity at 43 to 50% CO conversion.
[g] CO_2 selectivity at 43 to 50% CO conversion.
[h] Olefin/paraffin ratio at 43 to 50% CO conversion.
[i] The catalyst was impregnated with pure water, dried, and calcined. This was done to mimic the preparation procedure of the other catalysts, but impurities were carefully avoided.

Each experiment was divided into two periods of approximately 24 and 76 h in length. The following conditions were used:

Period 1 (0–25 h): Synthesis gas at either GHSV = 15,000 Nml/(g_{cat} h) (for 20 wt.% catalysts) or GHSV = 9000 Nml/(g_{cat} h) (for 12 wt.% catalysts).

Period 2 (25–100 h): Synthesis gas at an adjusted GHSV to give an initial target CO conversion of 50%. The adjusted GHSV depends on the CO conversion level in period 1 and will vary for each catalyst.

Heavy hydrocarbons were collected in a heated trap (85–95 °C), and liquid products were collected in a cold trap (25 °C). The effluent gaseous mixtures were analysed with an on-line GC (Agilent 6890) equipped with thermal conductivity (TC) and flame ionisation (FI) detectors.

CO reaction rates, turnover frequencies, and selectivity data were obtained after 100 h on stream. The turnover frequency based on hydrogen chemisorption data was calculated from:

$$TOF_{H2} = -r_{CO} \cdot M_{Co}/(D_{Co} \cdot x_{Co})$$

where $-r_{CO}$ is the CO reaction rate, M_{Co} is the atomic weight of cobalt, D_{Co} is the cobalt dispersion, and x_{Co} is the weight fraction of cobalt in the catalyst.

2.3.2. Fischer–Tropsch synthesis with the addition of sulphur- and nitrogen-containing compounds

In three separate experiments, H_2S, $(CH_3)_2S$, and NH_3 were introduced to the reactor in order to study the effect of S and N on cobalt-based catalysts. Common for all these experiments is two initial periods where no S or N was added to the catalysts. This was done in the same manner as described in Section 2.3.1. In the following period, S and N were added in varying amounts (0–10 ppm). For the H_2S experiment, the flow of S was controlled by co-feeding pure synthesis gas and H_2S-containing synthesis gas (20 ppm S). For the $(CH_3)_2S$ and NH_3 experiments, the flow of S and N, respectively, was controlled by co-feeding pure synthesis gas and $(CH_3)_2S$ and NH_3 containing helium (40 ppm S and 17 ppm N, respectively). The gas mixtures did not contain any unwanted impurities. In order to keep the partial pressures of H_2 and CO constant when $(CH_3)_2S$ and NH_3 were introduced, the reactor pressure was increased (22.9 bar for the $(CH_3)_2S$ experiment and 22.2 bar for the NH_3 experiment).

An *operando* dispersion was measured in the H_2S addition experiment. The dispersion value at the start of sulphur addition was calculated. The calculation was based on a one-to-one blocking model (i.e. one sulphur atom covers one cobalt atom). The number of cobalt atoms present on the surface at the time of

sulphur addition was calculated in part from the linear decrease in reaction rate during sulphur addition. The non-sulphur-related deactivation during sulphur addition was taken into account.

To ensure that adsorption of nitrogen and sulphur-containing compounds was minimal, a reference catalyst with known performance was run before and after every run with sulphur or nitrogen. The catalyst did not show any variability, and we consider any technical problem with the experiments to be negligible.

3. Results and discussion

The effect of impurity elements was investigated in two different ways. First, the effect of Na, K, Mg, Ca, Mn, Fe, P, and Cl was investigated *ex situ*. These elements were incorporated into the catalyst by impregnation. Second, the effect of S and N was investigated *in situ*. These elements were present in the synthesis gas feed to the catalyst. The *ex situ* work is described in Sections 3.1 to 3.5 and the *in situ* work in Sections 3.6–3.8.

3.1. Effect of alkaline earth metals (Ca, Mg)

In total, eight catalysts were prepared in order to investigate the effect of calcium on the catalytic performance. Three different supports were represented among the eight catalysts, γ-Al_2O_3 (Series 1), SiO_2 (Series 2), and $NiAl_2O_4$ (Series 5).

As already mentioned, Ca may come from various sources, e.g. synthesis gas precursor, refractory or ceramic liner in the synthesis gas section of the BTL plant, impure washing or impregnation water, the support, metal precursors, and process equipment. In order to simulate such impurity pick-up by the catalyst, a Ca precursor was introduced to the catalyst systems in quantities ranging from 100 to 1000 ppmw. Such a concentration range is attainable over 20,000 h (2.5 years) if the productivity is 1 kg hydrocarbons/(kg_{cat}·h), the synthesis gas contains 5–50 ppbw Ca, and all Ca in the synthesis gas is picked up by the catalyst. Thus, comparably, synthesis gases were simulated. A catalyst life time of 20,000 h and a productivity of 1 kg hydrocarbons/(kg_{cat} h) may be considered relevant for a modern XTL plant.

Characterisation data in Table 1 show that there were no morphological changes in the catalyst systems upon Ca introduction. Both the surface areas and pore volumes were, within experimental error, constant for all series of catalysts. Furthermore, hydrogen chemisorption did not reveal any variations in cobalt surface area. The same conclusion could be drawn from the propene chemisorption data. The amount of chemisorbed propene is expected to be directly proportional to cobalt surface area [29]. Fig. 1 illustrates the correlation between hydrogen and propene chemisorption data for all catalysts included in this work. A regression line through origin gives an excellent fit and a gradient of 0.49. This means that propene will occupy four times as many cobalt sites as a hydrogen atom. Apparently, the olefin–cobalt bond and the auxiliary hydrogens and the methyl group of propene give an average coverage of four cobalt atoms as the surface becomes saturated with propene. Thus, from two independent sets of measurements, the accessible cobalt surface area was found to be constant for the unmodified and Ca-modified catalysts. This should normally give a constant Fischer–Tropsch synthesis activity, provided that the cobalt particle size is larger than 6 nm [31]. As shown in Fig. 2, however, the Fischer–Tropsch synthesis activity (as measured after 100 h) decreased steadily as the amount of added Ca increased for the γ-Al_2O_3-based catalysts (■). For instance, at 1000 ppmw (0.22 mol%), the activity approached half of the activity of the unmodified catalyst. It should be noted that there were no variations in deactivation rates for the different catalysts. Thus, the effect of Ca was present initially.

Similar effects were observed for the SiO_2- and $NiAl_2O_4$-based catalysts. The presence of 500 ppmw (0.07 mol%) Ca in the CoRe/SiO_2 catalyst system and the presence of 400 ppmw (0.12 mol%) in the CoRe/$NiAl_2O_4$ catalyst system decreased the activity by 67% and 41%, respectively. Silica-supported catalysts appear more affected than the others, whereas $NiAl_2O_4$ seems more robust in the light of the lower surface areas available of both the support and cobalt. To conclude, the qualitative effect of Ca is independent of support, but the magnitude of the effect can vary from one catalyst system to another.

Since the activity decreased with Ca addition while the cobalt surface area was constant, the apparent turnover frequency decreased with increasing Ca content, see Table 1. The turnover frequencies are based on hydrogen chemisorption data. Turnover frequencies based on propene chemisorption data are not given as these would give exactly the same trend within the catalyst series, see Fig. 1. Strictly speaking, the term turnover frequency is misleading as the number of sites is measured *ex situ* under a non-reactive Fischer–Tropsch gaseous environment. Nevertheless, there may be several reasons why the activity decreased when Ca was present in the catalyst system.

Physical blocking of active cobalt sites by Ca is one possibility. However, it is unlikely that physical blocking is responsible for the activity decline as the quantity of Ca most likely is too small.

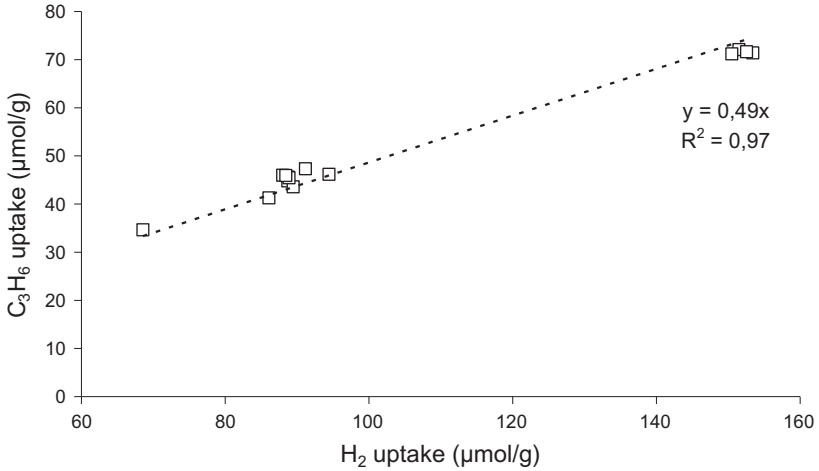

Fig. 1. Propene uptake vs. hydrogen uptake. The catalysts were reduced *in situ* at 350 °C for 16 h before chemisorption measurement. Propene and hydrogen chemisorption were done at 50 and 40 °C, respectively.

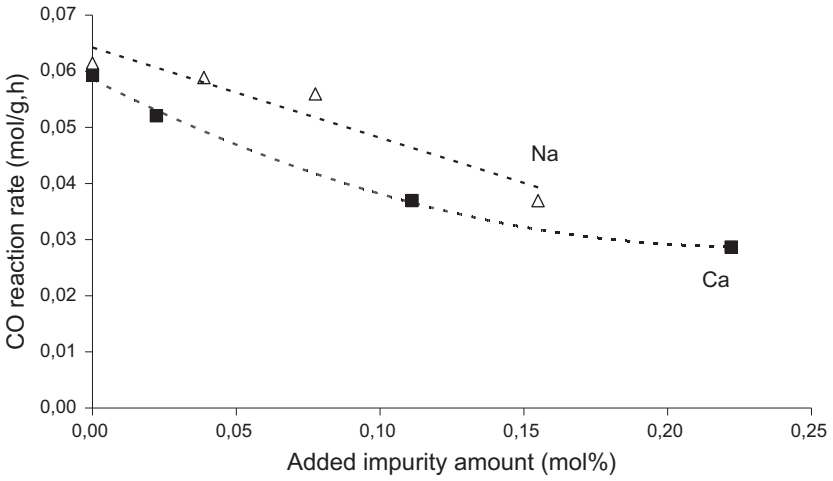

Fig. 2. CO reaction rate for calcium (Series 1) and sodium (Series 3)-modified γ-Al_2O_3-supported cobalt catalysts. The CO reaction rates were recorded after 100 h on stream at 483 K, 20 bar, and $H_2/CO = 2.1$ and the catalysts contained 20 wt.% Co and 0.5 wt.% Re.

In fact, if it is assumed that all added Ca atoms are present on the cobalt surface, that one Ca atom covers one cobalt atom, and that the activity can be directly deduced from the number of available cobalt atoms, the predicted normalised activity at 1000 ppmw is as high as 0.90. Clearly, the actual decrease is far larger (observed normalised activity is 0.48) and cannot be explained by a simple one-to-one blocking model. Note also that the calculated value of 0.90 represents an extreme scenario. If Ca adsorbs on the entire catalyst surface, the predicted normalised activity due to blocking will be even higher (e.g. for 1000 ppmw, the relative activity should be 0.99 if all available surface on the support and cobalt is covered proportionally). Taking also into account the constant chemisorption data, we conclude that site blockage is not the reason for the strong negative effect of Ca on activity.

Particle size effects are a second possible reason for the decrease in activity with Ca addition. It can be speculated that Ca introduction reduces the cobalt metal particle size to a region where the size influences activity [31]. For this reason, the cobalt particle size was calculated by combining the degree of reduction with hydrogen chemisorption data. For the catalysts of Series 1, the degree of reduction ranged from 65% to 77% which in combination with hydrogen chemisorption data gave a particle size range of 7.0–8.4 nm. This can be regarded as constant within the experimental errors of the measurements, and we conclude that particle size effects are not the reason for the low activity of the Ca-containing catalysts.

Electronic effects seem more likely to be responsible for the decrease in activity with Ca addition. Ca is electropositive and results in transfer of charge to the catalytic surface through the accompanying oxygen ion. According to Balonek et al. [5], this changes the adsorption and dissociation properties of the reactants. The authors claimed that the observed decrease in activity upon addition of Li, Na, K, and Ca to a CoRe/γ-Al_2O_3 catalyst was a result of decreased surface hydrogen concentrations and increased CO adsorption and dissociation. It was recently confirmed by SSITKA experiments that CO dissociation is largely enhanced when sodium is added to a CoRe/alumina catalyst [32]. Thus, carbon deposition may also play a role. As will be illustrated in Section 3.2, Na has the same effect on catalyst activity as Ca. It should be noted, however, that the alkali or alkaline earth impurities of the reduced catalyst still have to be present in the oxide state. The specific location of these elements has not been revealed. We will at this point, therefore, refrain from speculations on the detailed nature of a possible electronic effect.

Table 1 gives the C_{5+} and CO_2 selectivity values for the Ca-modified catalysts. The selectivity was evaluated at approximately constant CO conversion and, accordingly, the same water partial pressure as it is known that the conversion level has a strong effect on the selectivity [4]. As shown in Fig. 3, there is a linear relationship between the C_{5+} selectivity and the individual C_1–C_4 hydrocarbon selectivities for all catalysts. This figure represents both a slight decrease in chain-growth probability as the Ca level increases as well as the effect of deactivation within each activity test. The linearity observed implies that all individual selectivities are interrelated, even the methane formation which normally does not follow the Anderson–Schulz–Flory plot. The present observations are consistent with the recent work of Lögdberg et al. [33] where a large number of catalysts with different selectivities are compared. Further, Ca reduced the C_3 olefin/paraffin ratio as shown in Table 1. The reason was not lower propene selectivity and higher propane selectivity. In fact, both increased, but the propene selectivity increased less than the propane selectivity. The same trends were found for C_4 hydrocarbons. It is likely that Ca either increases the termination rate by hydrogenation to paraffins to a greater extent than it increases the termination rate to olefins, or secondary hydrogenation of olefins is promoted.

As shown in Table 1, the CO_2 selectivity increased with increasing Ca concentrations at a constant conversion level. Thus, the presence of calcium (oxide) enhances the water–gas-shift reaction, but the effect is small, and the produced hydrogen can hardly be the origin of the lower hydrocarbon selectivity.

The effect of magnesium was also investigated. As shown in Table 1, magnesium lowered the activity when added to CoRe/$NiAl_2O_4$, but the decrease (observed normalised activity 0.90) was significantly smaller than for Ca (observed normalised activity 0.59) although the molar percentage of Mg was higher than for Ca. This decrease in activity cannot rigorously be ascribed to other effects than physical blocking as the number of atoms added is sufficient to explain the activity decline by physical blocking of cobalt sites. Nevertheless, it is clear that alkaline earth metals decrease activity irrespective of support nature, and they should therefore be avoided in all steps of Fischer–Tropsch catalyst manufacture and use. This conclusion is furthered strengthened by the negative effect of magnesium on C_{5+} selectivity, see Table 1.

3.2. Effect of alkali metals (Na, K)

A similar study to that described in Section 3.1 was conducted for Na-spiked materials. In this context, Na may originate from

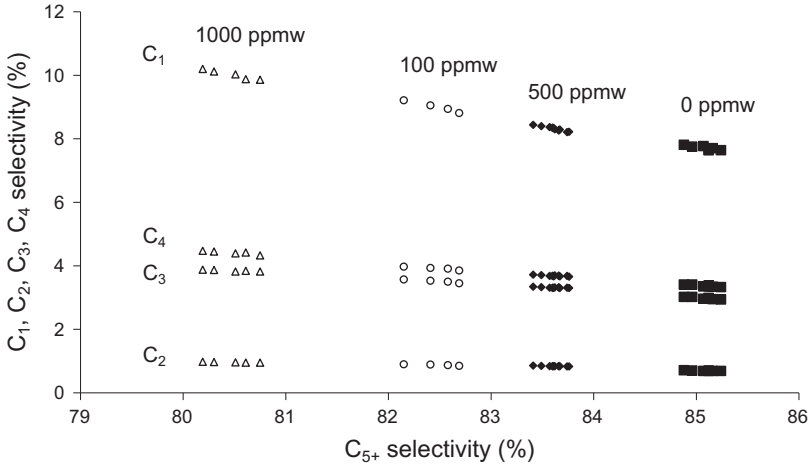

Fig. 3. C_1–C_4 selectivity versus C_{5+} selectivity for Ca-modified γ-Al_2O_3 supported cobalt catalysts (Series 1). Fischer–Tropsch synthesis was run at 483 K, 20 bar, and H_2/CO = 2.1 and the catalysts contained 20 wt.% Co and 0.5 wt.% Re.

the same sources as Ca. The effect of Na was investigated over γ-Al_2O_3 (Series 3), TiO_2 (Series 4), and $NiAl_2O_4$ (Series 5). The quantity of added Na ranged from 100 to 400 ppmw which corresponds to 5 to 20 ppbw of Na in the synthesis gas with the earlier-mentioned assumptions.

As the effects were qualitatively the same on all three catalyst systems, only the γ-Al_2O_3 based catalysts are commented on here. Data for the TiO_2- and $NiAl_2O_4$-based catalysts can be found in Table 1. Fig. 2 shows that the Fischer–Tropsch synthesis activity decreased as the Na concentration increased (Δ). At 400 ppmw, the activity was only 60% of the activity of the unmodified catalyst. Fig. 2 also shows that on a molar basis, the effect of Na is slightly weaker than the effect of Ca. Borg et al. [4] also found a negative correlation between the Na amount (20–120 ppm) and the activity of CoRe/γ-Al_2O_3. In their investigation, Na was not added to the catalyst system but was inherently present in the supports. The results in this investigation also agree with the investigations by Balonek et al. [5] and Gaube and Klein [6]. As for Ca, the decrease in activity due to Na addition is much larger than predicted if a one-to-one blocking model is assumed. Such a model would only give a predicted decrease in reaction rate of 6% at 400 ppmw. As mentioned earlier, electronic effects are possibly responsible for the observed effects. As shown in Fig. 4, Na has a similar electronegativity (Pauling type) as Ca and a similar effect on turnover frequency. All elements in Fig. 4 are present in concentrations ranging from 0.12–0.21 mol%, and the support is in all cases $NiAl_2O_4$ (Series 5).

In contrast to the negative impact on selectivity for Ca, the C_{5+} selectivity actually increased when Na was incorporated into the catalyst system. This is in agreement with Eri et al. [3] who found a higher chain-growth probability for alkali metals, but in contrast to the investigation by Gaube and Klein [6]. Both a lower methane selectivity and lower selectivity to individual C_2–C_4 hydrocarbons contributed to the higher C_{5+} selectivity. A reduced hydrogen concentration, as suggested by Balonek et al. [5], can explain the effect of Na on the long-chain hydrocarbon selectivity, but it is surprising that alkali and alkaline earth elements have opposite effects on the selectivity.

The CO_2 selectivity followed the same trend as for Ca, but the olefin/paraffin ratio increased with increasing Na concentration. Gaube and Klein [6] attributed their observed increase in 1-alkene selectivity to increased adsorption strength of carbon monoxide causing an enhanced displacement of 1-alkenes. The hypothesis of reduced propensity towards hydrogenation was ruled out. We are at variance with their interpretation as a high olefin/paraffin ratio follows a high C_{5+} selectivity for all alkali- and alkaline

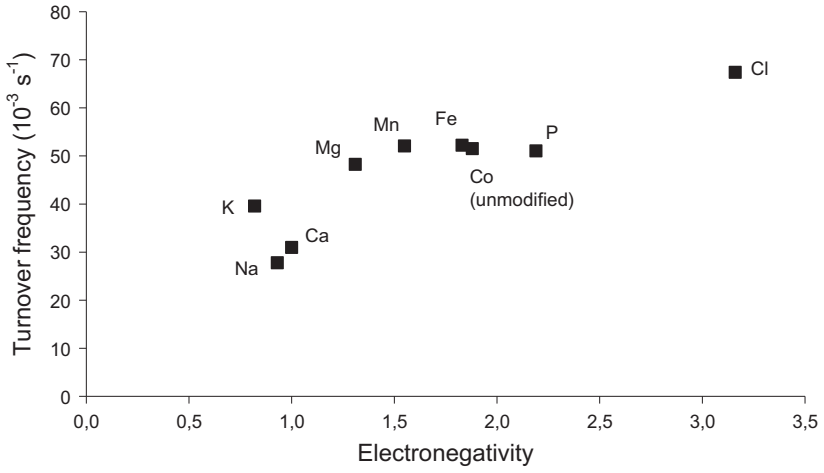

Fig. 4. Turnover frequency vs. element electronegativity (Pauling scale, Series 5). The turnover frequency is based on CO reaction rate after 100 h at 483 K, 20 bar, and H_2/CO = 2.1 and *ex situ* hydrogen chemisorption data obtained at 40 °C. All elements were present in concentrations ranging from 0.12 to 0.21 mol% and the support was in all cases $NiAl_2O_4$. The amount of Co and Re was 12 and 0.3 wt.%, respectively.

earth–modified catalysts. In other words, an apparent low propensity towards hydrogenation enhances the overall selectivity towards long-chain hydrocarbons. A similar trend was found for the effect of cobalt particle size [34].

As shown in Table 1, the potassium-modified catalyst worked similar to the Na-modified catalysts. To conclude, alkali metals slightly increase selectivity to heavy hydrocarbons but decrease the activity significantly.

3.3. Effect of Mn and Fe

Manganese and iron have both been tried as promoters in cobalt-based Fischer–Tropsch catalysts. However, the effect of small amounts has not been thoroughly investigated. Mn and Fe can be present as trace elements in biomass [35]. In this work, 400 ppmw Mn and 800 ppmw Fe were post-impregnated onto a $NiAl_2O_4$-supported cobalt catalyst. As shown in Table 1, these elements were not present in sufficient amounts to affect activity or selectivity.

3.4. Effect of P

Both hydrogen and propene chemisorption data showed that the accessible cobalt surface area was slightly lower for the phosphorus-modified catalyst than for the unmodified catalyst. The lower accessible surface area resulted in a proportionally lower normalised CO reaction rate (0.94). Thus, the turnover frequency was very close to the turnover frequency of the unmodified catalyst, see Fig. 4. It is, therefore, possible that P decreases activity by covering active cobalt sites. Based on the deviation between the expected activity from the number of P atoms added and the actual activity, one P atom seems to block less than one cobalt atom, possibly by also being present on the support. To conclude, there is a negative effect of P, but it must be emphasised that the catalyst tolerates a significantly greater quantity of P than of alkali and alkaline earth metals. The effect of P on product distribution was modest.

3.5. Effect of Cl

Chlorine is the only element in this investigation, which gave a significantly lower hydrogen and propene uptake than the unmodified catalyst when added in small amounts (ratio 0.75 and 0.73 for hydrogen and propene uptake, respectively, on the $NiAl_2O_4$-supported catalyst). A physical one-to-one blocking model based on the number of Cl atoms added gives a predicted normalised reaction rate of 0.62. The observed normalised CO reaction rate, however, was as high as 0.98, relative to the unmodified catalyst. Since, in this context, the measured cobalt surface area is low and the activity high, the apparent turnover frequency was higher than for the catalyst without any modification element. It is possible that Cl is removed from the cobalt surface during Fischer–Tropsch reaction, whereas the chemisorption conditions are not sufficiently severe to do the same. The issue of chlorine deserves further investigation. Surface-sensitive and chemical analysis techniques could give additional valuable information. However, surface techniques are challenging to carry out at relevant conditions, and chemical analysis does not give information about where the element is located (i.e. on the support or on the active cobalt phase). An additional electronic effect cannot be ruled out, see Fig. 4. The almost negligible effect of 800 ppmw Cl (40 ppbw in synthesis gas feed) on activity is surprising as a synthesis gas removal level as low as 10 ppbv for HCl, HBr, and HF has been recommended [2]. Neither an effect of Cl on product selectivity could be seen. The surprising non-harmful nature of Cl was confirmed on another catalyst system. As shown in Table 1 (Series 6), the presence of 1333 ppmw Cl in a CoRe/γ-Al_2O_3 catalyst system did not have a negative effect on the catalytic performance. In fact, the activity and C_{5+} selectivity of the Cl-modified catalyst were actually slightly higher than the activity and selectivity of the neat catalyst. In spite of the present observations on the effect of chloride impregnation, it will be interesting to study the direct *in situ* effect of chlorine compounds in the synthesis gas for a final verification of the non-harmful effect.

3.6. Effect of S on CoRe/$NiAl_2O_4$

Several sulphur-containing compounds can be present in the unpurified synthesis gas, in particular when the synthesis gas is based on a biomass feedstock. While the other investigated elements were introduced *ex situ* to the catalyst systems by impregnation, the effect of S on the catalyst was investigated *in situ* by introducing an H_2S- or $(CH_3)_2S$-containing synthesis gas. As mentioned in Section 2.3.2, a reference catalyst with known performance was run before and after every run to ensure no change in the rig lines. The catalyst used in all the *in situ* experiments is the unmodified catalyst of Series 5.

Although sulphur-containing compounds are known poisons for Fischer–Tropsch catalysts, the number of studies on cobalt-based catalysts is few. The impact of S seems to be complex and to depend strongly on the concentration. In a review of literature on cobalt deactivation, Tsakoumis et al. [36] pointed out that there is also a mismatch between conclusions drawn from *ex situ* and *in situ* investigations. S has been reported to both increase and decrease reaction rate. The effect of sulphur on C_{5+} selectivity is also controversial.

3.6.1. Effect of H_2S

Fig. 5 shows the CO reaction rate during the H_2S experiment. As described in Section 2.3.2, the experiment consisted of six different periods, in which S was present in three of them (third, fifth, and sixth period). In the first two periods (0–82 h), only non-sulphur-related deactivation took place. The reason for this deactivation is not well known nor is it the topic of this paper, but a recent review summarises the most likely causes [36]. Introduction of 2.5 ppmv S in the synthesis gas after 82 h induced a dramatic, linear decrease in reaction rate. This indicates a point-by-point physical blocking. After 85 h with S feeding (end of 2.5 ppmv period, 167 h on stream), approximately half of the activity had been lost. If all S was picked up by the catalyst, the catalyst would have contained 1600 ppmw at this point in time.

Pure synthesis gas was re-introduced after 168 h. The space velocity was adjusted to regain the initial 50% CO conversion. As shown in Fig. 5, the reaction rate was far lower than it was in period 2 where the CO conversion also initially was 50%. Thus, the catalyst had been deactivated irreversibly. Although it may be surprising that a slight positive step increase in the catalytic activity was observed when the S feed was stopped after 168 h, it does not necessarily mean that some S desorbed from the catalyst. Instead, we attribute the positive step change mainly to a kinetic effect resulting from increased water partial pressure. In fact, a similar step change is observed between the first and second period when the CO conversion was increased and adjusted to 50%.

Introduction of 4.8 and 9.5 ppmv S by H_2S (after 199 and 215 h) also led to a drop in reaction rate. For 9.5 ppmv, however, the decrease was not linear and levelled off as the rate approached zero. Such a saturation effect is regarded as normal. To summarise, there is no positive effect of S on the activity at low S levels, but a consistent negative effect at all concentration levels.

The linear decline in period 3 of Fig. 5 can be used to calculate an *operando* dispersion of cobalt at the onset of the period under the assumption that one S covers one Co, and therefore addresses the dilemma that standard dispersion methods operate under non-reactive conditions. The cobalt surface area obtained, 4.9 m^2/

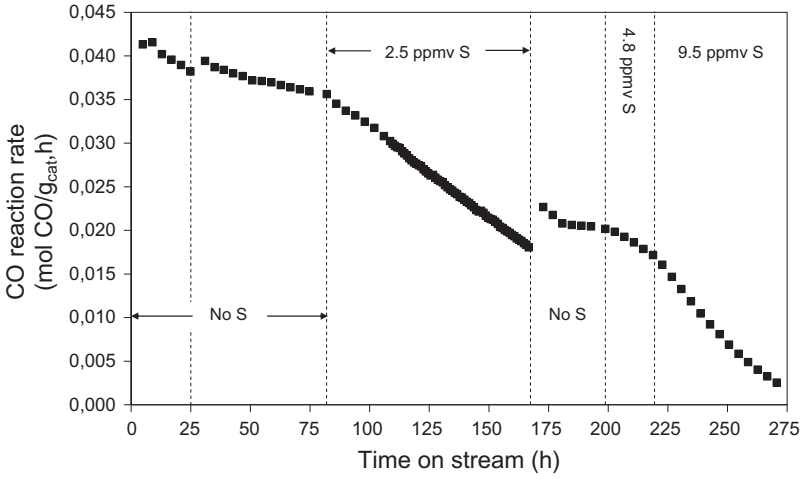

Fig. 5. CO reaction rate versus time on stream in the H_2S addition experiment. Fischer–Tropsch synthesis was run at 483 K, 20 bar, and $H_2/CO = 2.1$, and the catalyst composition was 12 wt.% Co/0.3 wt.% Re/$NiAl_2O_4$.

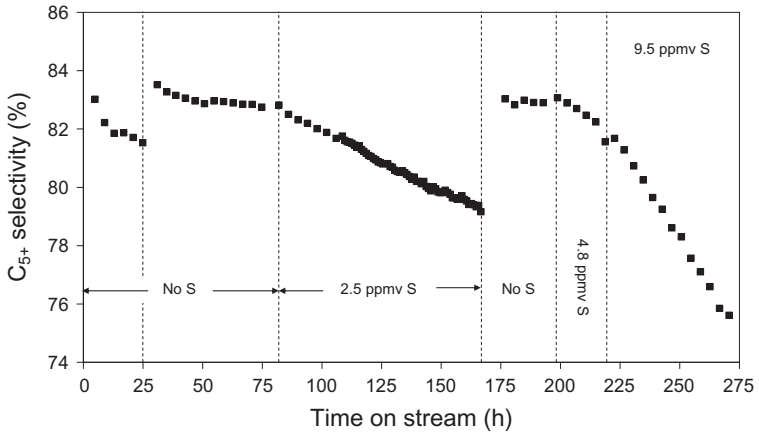

Fig. 6a. C_{5+} selectivity versus time on stream in the H_2S addition experiment. Fischer–Tropsch synthesis was run at 483 K, 20 bar, and $H_2/CO = 2.1$, and the catalyst composition was 12 wt.% Co/0.3 wt.% Re/$NiAl_2O_4$.

g, is definitely in the expected range and in good harmony with a slight decline from 7.3 m^2/g as found by hydrogen chemisorption of the fresh catalyst. To our knowledge, this is the first *operando* dispersion measurement reported for Fischer–Tropsch catalysts, and it both gives confidence to the standard hydrogen chemisorption method and supports a 1:1 stoichiometry of S on Co.

Establishing the effect of S on product selectivity is not as straightforward as establishing its effect on activity. In Fischer–Tropsch synthesis, the water partial pressure (dependent on CO conversion) has a significant effect on product selectivity [37]. Therefore, it is not surprising that the C_{5+} selectivity dropped sharply along with CO conversion when H_2S was introduced after 82 h, see Fig. 6a. Fig. 6b shows the C_{5+} selectivity in the different periods versus CO conversion level. Most data points lie on a straight line. There is a slight deviation from the straight-line behaviour in the last period (9.5 ppmv S, ○). It is not obvious whether it is the decreased CO conversion alone or the S addition contributes to the lower observed selectivity. The H_2S run was therefore compared with a separate run where no S was added, but the GHSV was varied to give different CO conversion levels and, accordingly, water concentrations. This run is labelled "GHSV experiment" (■) in Fig. 6b. The separate run clearly shows a linear trend between the CO conversion and C_{5+} selectivity similar to that observed for the H_2S run. In fact, the data points are overlapping. Thus, from these data, it is concluded that S does not affect the selectivity of C_{5+} hydrocarbons. It only affects the selectivity indirectly as it lowers the CO conversion and concurrently the water vapour pressure.

Similar results are evident for the CO_2 selectivity. The CO_2 selectivity increased as S was added, especially at high S loadings (not shown). However, if the separate control experiment and the CO conversion are taken into account, it is clear that S is not responsible, see Fig. 7. The separate experiment shows exactly the same trend between CO conversion and CO_2 selectivity. In addition, there is another surprising conclusion that follows from the analysis of the CO_2 data. The water–gas-shift reaction is normally expected to become more important at very high conversion levels where presumably some cobalt is reoxidised. Now, it is shown that a small, but still distinct, increase in CO_2 selectivity also occurs at low conversion levels (see "GHSV experiment" in Fig. 7). This CO_2 formation is not related to the water–gas-shift reaction as it is independent of S and is more pronounced at low partial pressures of water. Tentatively, we attribute this effect to direct oxidation of CO at the cobalt surface. As CO and hydrogen are adsorbed and dissociated on the surface, CH_x and OH_y intermediates are formed and further transformed to growing chains and water. For low conversion levels, the OH_y surface concentration will be reduced, and it is more preferred that oxygen atoms are available for CO oxidation.

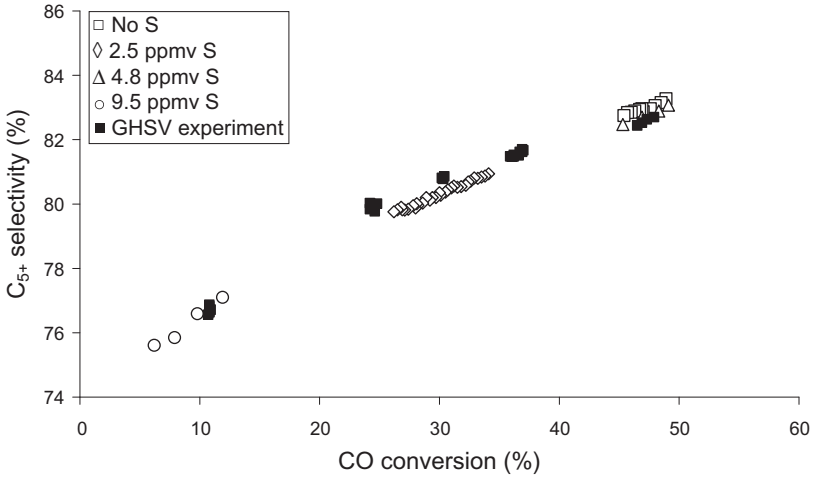

Fig. 6b. C_{5+} selectivity versus CO conversion in the H_2S addition experiment. Fischer–Tropsch synthesis was run at 483 K, 20 bar, and $H_2/CO = 2.1$, and the catalyst composition was 12 wt.% Co/0.3 wt.% Re/$NiAl_2O_4$.

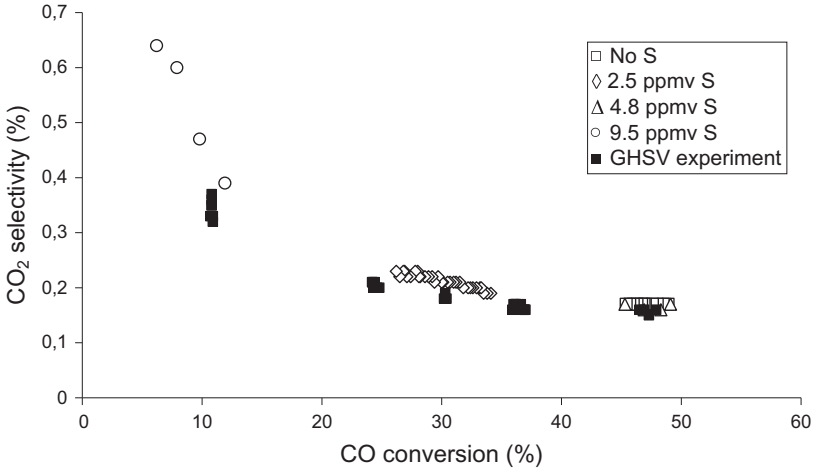

Fig. 7. CO_2 selectivity versus CO conversion in the H_2S addition experiment. Fischer–Tropsch synthesis was run at 483 K, 20 bar, and $H_2/CO = 2.1$, and the catalyst composition was 12 wt.% Co/0.3 wt.% Re/$NiAl_2O_4$.

An analogous discussion as for CO_2 is valid for the olefin/paraffin ratio. A slight deviation, however, in terms of influence of sulphur, can be inferred. By comparing periods 2 and 4 in Fig. 8, in which the CO conversion was similar, an effect of accumulated sulphur is seen. As S has no effect on activity and C_{5+} selectivity, sulphur does slightly enhance secondary hydrogenation of olefins. The present interpretation is not in agreement with the investigation of Visconti et al. [23] who concluded that an increased CO_2 selectivity and olefin/paraffin ratio observed at high S concentrations were results of enhanced water–gas-shift activity and suppression of olefin hydrogenation.

To summarise the H_2S experiment, S has a negative impact on activity at all concentrations, but it does not affect the product distribution, with a slight deviation for secondary olefin hydrogenation.

3.6.2. Effect of $(CH_3)_2S$

Fig. 9 shows the CO reaction rate during the $(CH_3)_2S$ experiment for the same catalyst as used in the H_2S experiment. Similar to the H_2S experiment described in the previous section, the experiment started with two periods without S feeding. The experimental details are described in Section 2.3.2. A synthesis gas containing 5.1 ppmv S was introduced after 49 h. This induced a steep drop in reaction rate. In fact, the catalyst was completely poisoned after only 18 h. At this point, the catalyst contained 1400 ppmw of S if all S was picked up by the catalyst. By comparing Figs. 5 and 9, it is clear that $(CH_3)_2S$ is more harmful than H_2S. If it is assumed that S from one H_2S molecule inhibits one cobalt atom from the Fischer–Tropsch reaction, it can be inferred that $(CH_3)_2S$ deactivates as much as six cobalt atoms from participating in Fischer–Tropsch synthesis. This is surprising as $(CH_3)_2S$ is known to dissociate to methane and H_2S on the catalytic surface. If this is the case, the effect of H_2S and $(CH_3)_2S$ should be similar. On the other hand, if $(CH_3)_2S$ does not dissociate on the catalytic surface, its strong deactivating effect could be related to the larger molecular size. The methyl groups may restrict reactant molecules to adsorb on cobalt sites more efficiently than the hydrogen atoms of the H_2S molecule. Further studies to understand the different effects of H_2S and $(CH_3)_2S$ should be conducted.

There is no effect of S on overall product selectivity in the $(CH_3)_2S$ experiment. Like the H_2S experiment, the CO_2 selectivity and olefin/paraffin ratio increased and the C_{5+} selectivity decreased (not shown) when S was present in the feed, but the changes can be explained by the progressively lower CO conversion levels.

3.7. Effect of NH_3 on $CoRe/NiAl_2O_4$

The effect of ammonia was evaluated *in situ* with an ammonia-containing synthesis gas. The catalyst used in the *in situ* experiment is the unmodified catalyst of Series 5. There was no change

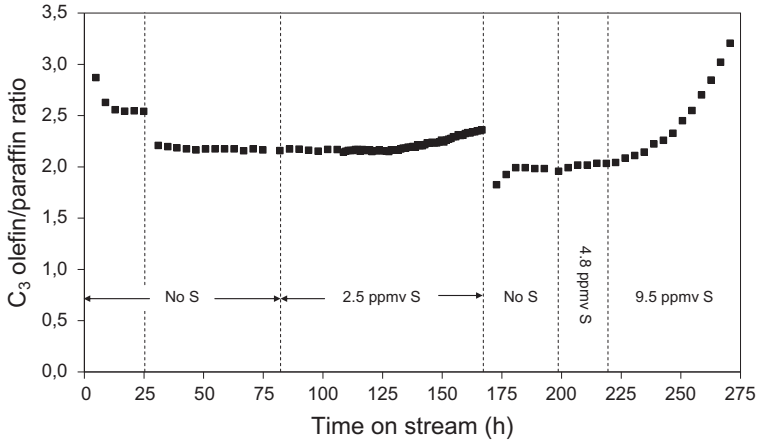

Fig. 8. C_3 olefin/paraffin ratio versus time on stream in the H_2S addition experiment. Fischer–Tropsch synthesis was run at 483 K, 20 bar, and $H_2/CO = 2.1$, and the catalyst composition was 12 wt.% Co/0.3 wt.% $Re/NiAl_2O_4$.

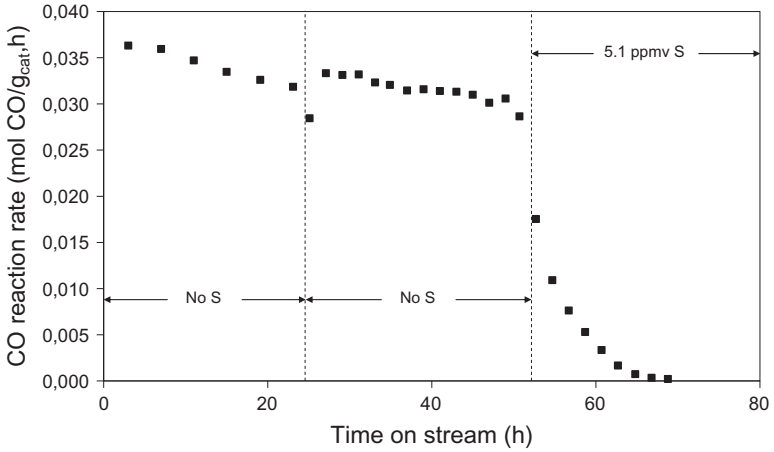

Fig. 9. CO reaction rate versus time on stream in the $(CH_3)_2S$ addition experiment. Fischer–Tropsch synthesis was run at 483 K, 20 bar, and $H_2/CO = 2.1$, and the catalyst composition was 12 wt.% Co/0.3 wt.% $Re/NiAl_2O_4$.

in activity when NH_3 (4.2 ppmv nitrogen) was added (not shown). This is in agreement with Claeys et al. [15] who demonstrated that co-feeding of up to 25% NH_3 in the synthesis gas did not affect the Fischer–Tropsch synthesis activity. The same conclusion could be drawn regarding the selectivity.

4. Conclusions

The main conclusions from the work are listed below:

- Alkali metals and alkaline earth metals dramatically decrease the activity of cobalt Fischer–Tropsch catalysts. The magnitude of the effects may differ for one catalyst system to another, but the qualitative effects are similar. Chemisorption is fairly unchanged, and an electronegativity effect is inferred.
- Surprisingly, chlorine does not lower the activity when present in moderate amounts in spite of significantly lower available cobalt surface area as found by chemisorption.
- Introduction of sulphur induces a point-by-point blocking of active sites. The number of sites blocked per molecule added is significantly higher (factor: 6) for $(CH_3)_2S$ than for H_2S.
- *Operando* dispersion measurements by H_2S are in good accordance with hydrogen and propene chemisorption of freshly reduced catalysts.
- Sulphur does not affect the primary Fischer–Tropsch synthesis product distribution but increases secondary hydrogenation of olefins.
- Small amounts of ammonia do not affect Fischer–Tropsch synthesis activity or selectivity.
- The CO_2 selectivity increases at low CO conversion levels, in contrast to what is expected from the water–gas-shift reaction.

Author contributions

- Dr. Øyvind Borg performed a major part of the characterisation experiments, was central in the interpretation of the data, and wrote the manuscript.
- Dr. Nina Hammer performed a major part of the characterisation experiments.
- Dr. Bjørn Christian Enger was central in the planning of the experiments.
- Rune Myrstad performed several of the Fischer-Tropsch tests.
- Odd Asbjørn Lindvåg performed several of the Fischer-Tropsch tests.
- Sigrid Eri was central in the interpretation of the activity/selectivity data.

- Torild Hulsund Skagseth prepared all the catalysts and performed a part of the characterisation experiments.
- Dr. Erling Rytter was central in all parts of the work; planning, interpretation of the data, and writing of the manuscript.

Acknowledgments

This publication forms a part of the inGAP Centre of Research-based Innovation, which receives financial support from the Norwegian Research Council under Contract no. 174893. GTL.F1 AG is acknowledged for releasing the material for publication.

References

[1] C.N. Hamelinck, A.P.C. Faaij, H. den Uil, H. Boerrigter, Energy 29 (2004) 1743.
[2] H. Boerrigter, H. den Uil, H.-P. Calis, Green diesel from biomass via Fischer–Tropsch synthesis: new insights in gas cleaning and process design, Paper, Pyrolysis and Gasification of Biomass and Waste Expert Meeting, Strasbourg, France,
[3] S. Eri, J.G. Goodwin Jr., G. Marcelin, T. Riis, US 4880,763, 1989 (to Den Norske Stats Oljeselskap AS).
[4] Ø. Borg, S. Eri, E.A. Blekkan, S. Storsæter, H. Wigum, E. Rytter, A. Holmen, J. Catal. 248 (2007) 89.
[5] C.M. Balonek, A.H. Lillebø, S. Rane, E. Rytter, L.D. Schmidt, A. Holmen, Catal. Lett. 138 (2010) 8.
[6] J. Gaube, H.-F. Klein, Appl. Catal. A 350 (2008) 126.
[7] C.H. Bartholomew, R.C. Reuel, Ind. Eng. Chem. Prod. Res. Dev. 24 (1985) 56.
[8] A. Guerrero-Ruiz, A. Sepúlveda-Escribano, I. Rodríguez-Ramos, Appl. Catal. A 120 (1994) 71.
[9] Y. Zhang, H. Xiong, K. Liew, J. Li, J. Mol. Catal. A 237 (2005) 172.
[10] F. Morales Cano, O.L.J. Gijzeman, F.M.F. de Groot, B.M. Weckhuysen, Stud. Surf. Sci. Catal. 147 (2004) 271.
[11] G.L. Bezemer, U. Falke, A.J. van Dillen, K.P. de Jong, Chem. Commun. (2005).
[12] D.J. Duvenhage, N.J. Coville, Appl. Catal. A 153 (1997) 43.
[13] S. Lögdberg, D. Tristantini, Ø. Borg, L. Ilver, B. Gevert, S. Järås, E.A. Blekkan, A. Holmen, Appl. Catal. B 89 (2008) 167.
[14] S.C. Levinnes, C.J. Mart, W.C. Behrmann, S.J. Hsia, D.R. Neskora, International Publication Number WO 98/50487, 1998 (to Exxon Research and Engineering Company).
[15] M. Claeys, E. van Steen, T. Sango, C. de Vries, R. Henke, A.K. Rausch, F. Roessner, Enhanced production of chemicals via co-feeding of ammonia during Fischer–Tropsch synthesis, Poster presentation, 9th Novel Gas Conversion Symposium, Lyon, France, 30 May–3 June 2010.
[16] W. Chao, K.M. Makar, L.E. Manzer, M.A. Subramanian, US 6489,371 B2, 2002 (to Conoco Inc.).
[17] M.C.J. Bradford, M. Te, A. Pollack, Appl. Catal. A 283 (2005) 39.
[18] J.W. Bae, S.-M. Kim, Y.-J. Lee, M.-J. Lee, K.-W. Jun, Catal. Commun. 10 (2009) 1358.
[19] C.H. Bartholomew, R.M. Bowman, Appl. Catal. 15 (1985) 59.
[20] A.L. Chaffee, I. Campbell, N. Valentine, Appl. Catal. 47 (1989) 253.
[21] V. Curtis, C.P. Nicolaides, N.J. Coville, D. Hildebrandt, D. Glasser, Catal. Today 49 (1999) 33.
[22] J. Li, N.J. Coville, Appl. Catal. A 208 (2001) 177.
[23] C.G. Visconti, L. Lietti, P. Forzatti, R. Zennaro, Appl. Catal. A 330 (2007) 49.
[24] S.S. Pansare, J.D. Allison, Appl. Catal. A 387 (2010) 224.
[25] A.G. Shastri, A.K. Datye, J. Schwank, Appl. Catal. 14 (1985) 119.
[26] S. Brunauer, P.H. Emmett, E. Teller, J. Am. Chem. Soc. 60 (1938) 309.
[27] E.P. Barrett, L.G. Joyner, P.P. Halenda, J. Am. Chem. Soc. 73 (1951) 373.
[28] S. Lowell, J.E. Shields, M.A. Thomas, M. Thomess, Characterization of Porous Solids and Powders: Surface Area, Pore Size and Density, Kluwer Academic Publishers, Dordrecht, 2004. p. 117.
[29] J.-S. Girardon, A.S. Lermontov, L. Gengembre, P.A. Chernavskii, A. Griboval-Constant, A.Y. Khodakov, J. Catal. 230 (2005) 339.
[30] C.H. Bartholomew, R.J. Farrauto, J. Catal. 45 (1976) 41.
[31] A. Barbier, A. Tuel, I. Arcon, A. Kodre, G.A. Martin, J. Catal. 200 (2001) 106.
[32] J. Yang, A.H. Lillebø, D. Chen, A. Holmen, Effect of ppm level sodium on CoRe/Al_2O_3 catalyst for the Fischer–Tropsch reaction studied by SSITKA, Poster presentation, 9th Novel Gas Conversion Symposium, Lyon, France, 30 May–3 June 2010.
[33] S. Lögdberg, M. Lualdi, S. Järås, J.C. Walmsley, E.A. Blekkan, E. Rytter, A. Holmen, J. Catal. 274 (2010) 84.
[34] Ø. Borg, P.D.C. Dietzel, A.I. Spjelkavik, E.Z. Tveten, J.C. Walmsley, S. Diplas, S. Eri, A. Holmen, E. Rytter, J. Catal. 259 (2008) 161.
[35] Z. Gogebakan, N. Selçuk, J. Hazard. Mater. 162 (2009) 1129.
[36] N.E. Tsakoumis, M. Rønning, Ø. Borg, E. Rytter, A. Holmen, Catal. Today 154 (2010) 162.
[37] E.A. Blekkan, Ø. Borg, V. Frøseth, A. Holmen, Roy. Soc. Chem., Catal. 20 (2007) 13.